

Reconstructing singly produced top partners in decays to Wb

 Nicolas Gutierrez,¹ James Ferrando,¹ Deepak Kar,¹ and Michael Spannowsky²
¹*School of Physics and Astronomy, University of Glasgow, Glasgow G12 8QQ, United Kingdom*
²*Department of Physics, Institute for Particle Physics Phenomenology, Durham University, Durham DH1 3LE, United Kingdom*

(Received 11 June 2014; published 14 October 2014)

Fermionic top partners are a feature of many models of physics beyond the standard model. We propose a search strategy for single production of top partners focusing specifically on the dominant decay to Wb . The enormous background can be reduced by exploiting jet substructure to suppress top-pair production and by requiring a forward jet. This simple strategy is shown to produce a sensitive search for single top-partner production, in the context of composite Higgs models, that has competitive mass reach with existing experimental searches for top-partner-pair production at the 8 TeV LHC.

DOI: 10.1103/PhysRevD.90.075009

PACS numbers: 12.60.-i

I. CONTEXT AND INTRODUCTORY REMARKS

With the observation of a standard model-like Higgs boson [1,2] at the LHC, our understanding of electroweak symmetry breaking has been significantly enhanced. The attention of experiments at the LHC now turns to establishing the properties of this new resonance. The possibility that the resonance is actually a composite bound state remains open, and in this work we study a top partner search in the context of composite Higgs scenarios [3–9]. The discovery of such top partners would spectacularly elucidate the mechanism by which the scalar resonance mass is stabilized at the electroweak scale.

Although the Higgs boson can be a generic composite bound state, we focus on the realization of the Higgs boson as a pseudo-Nambu-Goldstone boson (pNGB) of the coset G/H , G is an approximate global symmetry and H is an unbroken subgroup. We assume partial compositeness [4] to evade flavor physics constraints [10]. Here, the standard model (SM) fermions obtain masses via mixing with composite bound states from the strongly coupled sector. Since SM fermions arise as admixtures of the elementary and the corresponding composite bound states, there are necessarily accompanying heavy excitations with the same SM quantum numbers, so-called top partners. They belong to a representation of the unbroken subgroup H .

Following Ref. [11] we adopt a minimal setup for $G = SO(5) \times U(1)_X$ and $H = SO(4) \times U(1)_X$. We assume t_R to be a completely composite chiral state and only $q_L = (b, t)_L$ to be partially composite. In this short article we focus on evaluating the LHC sensitivity for discovering or excluding a top partner belonging to the singlet $\Psi = \mathbf{1}_{2/3}$ of the unbroken $SO(4)$. The operators \mathcal{O} induced by the interactions of the fermions in the strong sector are assumed to transform in the representation $r_{\mathcal{O}} = 5_{2/3}$.¹

¹Our results can be interpreted straightforwardly if the operators \mathcal{O} of the strong-sector fermions transform in the representation $r_{\mathcal{O}} = \mathbf{14}_{2/3}$.

The interaction Lagrangian for \tilde{T} is given by

$$\mathcal{L} = \mathcal{L}_{\text{kin}} - M_{\Psi} \bar{\Psi} \Psi + [y f (\bar{Q}_L^5)^I U_{I5} \Psi_R + y c_2 f (\bar{Q}_L^5)^I U_{I5} t_R + \text{H.c.}] \quad (1)$$

and the mass eigenvalue of the top partner \tilde{T} is approximately given by

$$m_{\tilde{T}} \simeq M_{\Psi} \left[1 + \frac{y^2}{4g_{\Psi}^2} \frac{v^2}{f^2} \right], \quad (2)$$

where $v = 246$ GeV and $g_{\Psi} = M_{\Psi}/f$.

As a result, the phenomenology of \tilde{T} is determined by four parameters: (M_{Ψ}, y, c_2, f) . M_{Ψ} is the mass of the top partner, y controls the mixing between the composite and elementary states, c_2 is an $\mathcal{O}(1)$ parameter associated with the interactions of t_R and f is the symmetry breaking scale of the strong sector. By requiring the four parameters to conspire to give the observed top quark mass, one degree of freedom in this parameter space can be removed, i.e. we choose $y = 1$. In the following quantitative analysis we also choose $\xi = \frac{v^2}{f^2} = 0.2$ to ensure compatibility with electroweak precision tests [12–14]. The cross section also depends on the parameter c_2 , as described in Ref. [11]. Here we choose $c_2 = 0.891767$ for a \tilde{T} mass of 700 GeV.

Pair production of fermionic top partners has been thoroughly searched for at the LHC [15,16]. In composite Higgs models, light top partners are well motivated [17] but so far masses less than 687–782 GeV have been excluded depending on the branching ratio to different final states. In this work, we focus instead on single production: $pp \rightarrow q\tilde{T}b$. The cross section for single production is smaller than that for pair production at low masses of the top partner. However, depending on the weak coupling to the top partner, single production can begin to have a larger cross section in the mass-range of 600–1000 GeV [18]. Thus, well-designed searches for single production can potentially extend the mass-reach of the LHC experiments.

Singlet top partners decay to Wb , tZ or tH in the approximate ratio 2:1:1, respectively, and the significant branching fractions to tZ and tH have attracted previous attention [11,19,20]. In particular, multileptonic final states arising from these decays make for searches with low background, albeit at a relatively low overall signal efficiency. Here, we have chosen to focus on the most abundant expected decay: $\tilde{T} \rightarrow Wb$, with subsequent decay of the W boson to leptons.² Trading a clean final state for a larger signal efficiency can be beneficial for large top partner masses [22]. The present experimental limits are weakest for large values of the $\tilde{T} \rightarrow Wb$ branching ratio [16]. We demonstrate that, by requiring a forward jet and exploiting jet substructure to suppress backgrounds from top-quark production, this relatively neglected channel can become a promising one for discovery of single top-partner production at the LHC.

II. ELEMENTS OF THE ANALYSIS

A. Samples

Signal events were simulated using MADGRAPH5 [23] interfaced with PYTHIA 8.185 [24] for parton-shower and fragmentation. For a top partner with mass 700 GeV, the leading-order cross sections from MADGRAPH are 0.163 pb (0.957 pb) for $\sqrt{s} = 8$ TeV (14 TeV).³ Background samples of $t\bar{t}$ and $W + \text{jets}$ were generated with up to two and four additional partons using SHERPA [25] 2.1.0. Single top quark production in the t -channel was modeled, in a four-flavor scheme [26], using POWHEG-BOX [27] showered with PYTHIA 8.185.

The $t\bar{t}$ production cross section of the SHERPA sample was scaled to the next-to-next-to-leading-order prediction including resummation of next-to-next-to-leading logarithmic soft gluon terms [28] calculated using the NNPDF2.3 PDF set [29]. Approximate corrections to next-to-leading order for the signal cross-section were calculated using the single-top cross section from POWHEG-BOX, with the top-mass set to the mass of the top-partner compared to the equivalent leading order cross-section calculated from MADGRAPH. These corrections to the signal were approximately 14(7)% for 8(14) TeV.

B. Event selection and top-partner reconstruction

Analysis of the samples of simulated events is performed on the stable final-state particles using RIVET 2.1.1 [30]. The event selection was designed to select singly produced \tilde{T} quarks with subsequent $\tilde{T} \rightarrow Wb$ decay. For leptonically decaying W -bosons, the signal event topology is characterized by a charged lepton, missing

²This final state could also be used to search for exotic bottom partners [21], although we do not consider that possibility here.

³The branching ratio $\tilde{T} \rightarrow Wb$ for our parameter choices is 0.55.

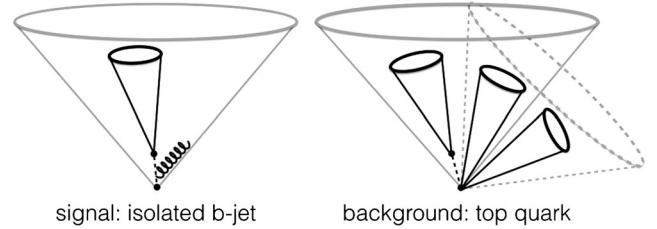


FIG. 1. Illustration of the usage of large-radius jet mass to veto $t\bar{t}$ background. For the signal $\tilde{T} \rightarrow Wb$, the b -quark recoils against the W -boson. Thus the hardest large-radius jet in the event typically contains a b -hadron plus additional soft and collinear radiation, and tends to have a low mass. For the semileptonic $t\bar{t}$ background, right, a mildly boosted hadronically decaying top quark produces large-radius jets containing a significant fraction of the top decay products. The fraction of top decay products contained, and therefore the jet mass, increases with jet p_T . Hence, after requiring a matching between a small-radius b -jet and large-radius jet, a cut based on the large-radius jet p_T and mass can be optimized to distinguish between signal and $t\bar{t}$ background, whilst still retaining good signal efficiency.

transverse momentum, a high- p_T b -tagged central jet and a forward jet.

Final-state electrons are corrected for energy loss due to photon emission by combining them with all final-state photons within $\Delta R(e, \gamma) < 0.1$, where $\Delta R(e, \gamma)$ is the distance in the η - ϕ plane between the electron and the photon. Charged leptons are required to be isolated from other particles.⁴ The typical fiducial acceptance of the ATLAS detector [32] is mimicked by only using electrons with $1.52 < |\eta| < 2.47$ or $|\eta| < 1.37$, and muons with $|\eta| < 2.5$.

Small-radius jets are clustered from all final-state particles with $|\eta| < 5.0$, except muons and neutrinos, using the anti- k_r algorithm [33,34] with a radius parameter of 0.4. Only jets with $p_T \geq 25$ GeV for $|\eta| < 2.4$ or $p_T \geq 35$ GeV for $2.5 < |\eta| < 4.5$ are used. In order to account for electrons misidentified as small-radius jets, any small-radius jet (j) with $\Delta R(e, j) \leq 0.2$ are discarded. Large-radius jets are clustered in a similar manner, but with a radius parameter of 1.0. These large-radius jets were required to have $p_T \geq 100$ GeV and $|\eta| < 1.2$.

Jets are referred to as b -jets if their constituents contain a bottom flavored hadron or the decay products of at least one such hadron. The typical performance of experimental jet b -tagging was mimicked by ascribing a 0.7 probability for

⁴Isolation criteria that were similar to those used in an ATLAS same-sign dilepton search [31] were adopted. For electrons, the isolation requirement is that the total p_T of all charged particles (p_q), $\sum p_T$, with $\Delta R(e, p_q) < 0.3$ should be less than 10% of the electron p_T . Similarly for muons, $\sum p_T$ for all particles with $\Delta R(\mu, p) < 0.4$ is required to be less than 6% of the muon p_T , but in addition, $\sum p_T$ is required to be less than $4 + p_T \times 0.02$.

TABLE I. The number of expected events for an integrated luminosity of 20 fb^{-1} at the LHC with 8 and 14 TeV.

	Number of events					
	After preselection		After jet veto		After final selection	
	8 TeV	14 TeV	8 TeV	14 TeV	8 TeV	14 TeV
$W + \text{jets}$	40.1×10^6	87.3×10^6	391	1403.2	92	368.1
$t\bar{t}$	1.13×10^6	4.1×10^6	222.1	887	32	217.7
Single top	2176.8	25981	28	380	13	223.2
Total background	41.3×10^6	91.4×10^6	640.6	2670	137	809
Signal ($m(\tilde{T}) = 700 \text{ GeV}$)	664.5	3653	54.4	234.3	30	161
S/B	1.61×10^{-5}	4×10^6	0.085	0.088	0.22	0.20
S/\sqrt{B}	0.1	0.38	2.15	4.53	2.5	5.65

tagging b -jets and a 0.01 mistag rate for b -tagging jets from other sources [35].

The missing transverse momentum, E_T^{miss} , is the magnitude of the total transverse momentum calculated from all final-state particles with $|\eta| < 5.0$ except neutrinos. The missing transverse momentum direction is defined as being directly opposite to this same total transverse momentum.

Events are preselected by requiring exactly one electron or muon with $p_T \geq 25 \text{ GeV}$, $E_T^{\text{miss}} \geq 20 \text{ GeV}$ and E_T^{miss} plus transverse mass⁵ of 60 GeV. Events are also required to contain at least two small-radius jets and at least one large-radius jet with $p_T > 200 \text{ GeV}$. After this selection, the dominant background processes are $W + \text{jet}$ production and $t\bar{t}$ production. Further cuts were applied with the goal of optimizing the statistical significance S/\sqrt{B} , defined as the number of 700 GeV top-partner signal (S) events divided by the square root of the number of background (B) events.

The $W + \text{jet}$ background is suppressed by requiring that a b -tagged small-radius jet is matched to the large-radius jet.⁶ The $t\bar{t}$ background is also suppressed by requiring that the large-radius jet have $p_T > 250 \text{ GeV}$ and mass $< 70 \text{ GeV}$. The latter requirement exploits the fact that high p_T large-radius jets in $t\bar{t}$ tend to have a genuinely large mass since they contain at least two decay products from $t \rightarrow Wb \rightarrow \bar{q}q'b$, as illustrated in Fig. 1. To ensure that the lepton is not within the active area of the large-radius jet, it is required that $\Delta\phi(l, \text{jet}) > 1.5$.

The expected isolation of the b -tagged jet from the \tilde{T} decay can be exploited further by vetoing events with extra central jets (those with $|\eta| < 2.4$) above a certain p_T threshold. Theoretical uncertainties when vetoing extra jets decrease for higher thresholds, i.e. the resummation of contributions $\sim \ln^2(\sqrt{\hat{s}}/p_{T,\text{veto}})$ becomes increasingly important for lower cutoff scales [36]. Hence, this cut was

⁵We define the transverse mass of the lepton and E_T^{miss} to be $m_T = \sqrt{2p_T^l E_T^{\text{miss}}(1 - \cos\phi_{l\nu})}$, where $\cos\phi_{l\nu}$ is the azimuthal angle between the charged lepton and the missing transverse momentum direction.

⁶Small radius jets are considered matched to large radius jets if their four vectors lie within an η - ϕ distance of 0.8.

optimized by looking for both the largest S/\sqrt{B} and the largest jet p_T threshold. The optimal threshold was found to be 75 GeV. Finally, events must have at least one jet with $p_T \geq 35 \text{ GeV}$ and $2.5 < |\eta| < 4.5$, consistent with the single top partner production mechanism.

In Table I, the number of expected events for 20 fb^{-1} integrated luminosity at the 8 TeV and 14 TeV LHC is shown at the preselection stage, after requiring the central jet-veto, and after the final selection. The selection cuts lead to a S/B of 0.22 (0.20) and S/\sqrt{B} of 2.5 (5.65) for a 700 GeV \tilde{T} at 8 TeV(14 TeV). The addition of the forward jet requirement leads to modest improvements in S/\sqrt{B} but more than doubles S/B , it can thus be very useful in the case of large experimental uncertainties on the background normalization.

To search for \tilde{T} production, a candidate \tilde{T} -mass constructed from the charged lepton and the b -jet and neutrino candidates is used. The b -tagged small-radius jet, that is matched to the large radius jet, is used as the b -jet candidate. The neutrino candidate is constructed from the E_T^{miss} and charged lepton by imposing a W -mass constraint on the lepton + E_T^{miss} system [35]. The resulting \tilde{T} -candidate mass distribution is shown for signal and backgrounds in Fig. 2 for

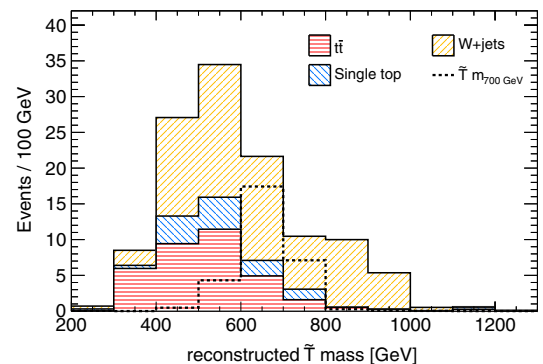


FIG. 2 (color online). The distribution of the \tilde{T} candidate mass used in the statistical analysis is shown for 20 fb^{-1} integrated luminosity at the 8 TeV LHC. The shape of the SM background from $W + \text{jets}$, $t\bar{t}$ and single top production are compared to the shape of the expected signal.

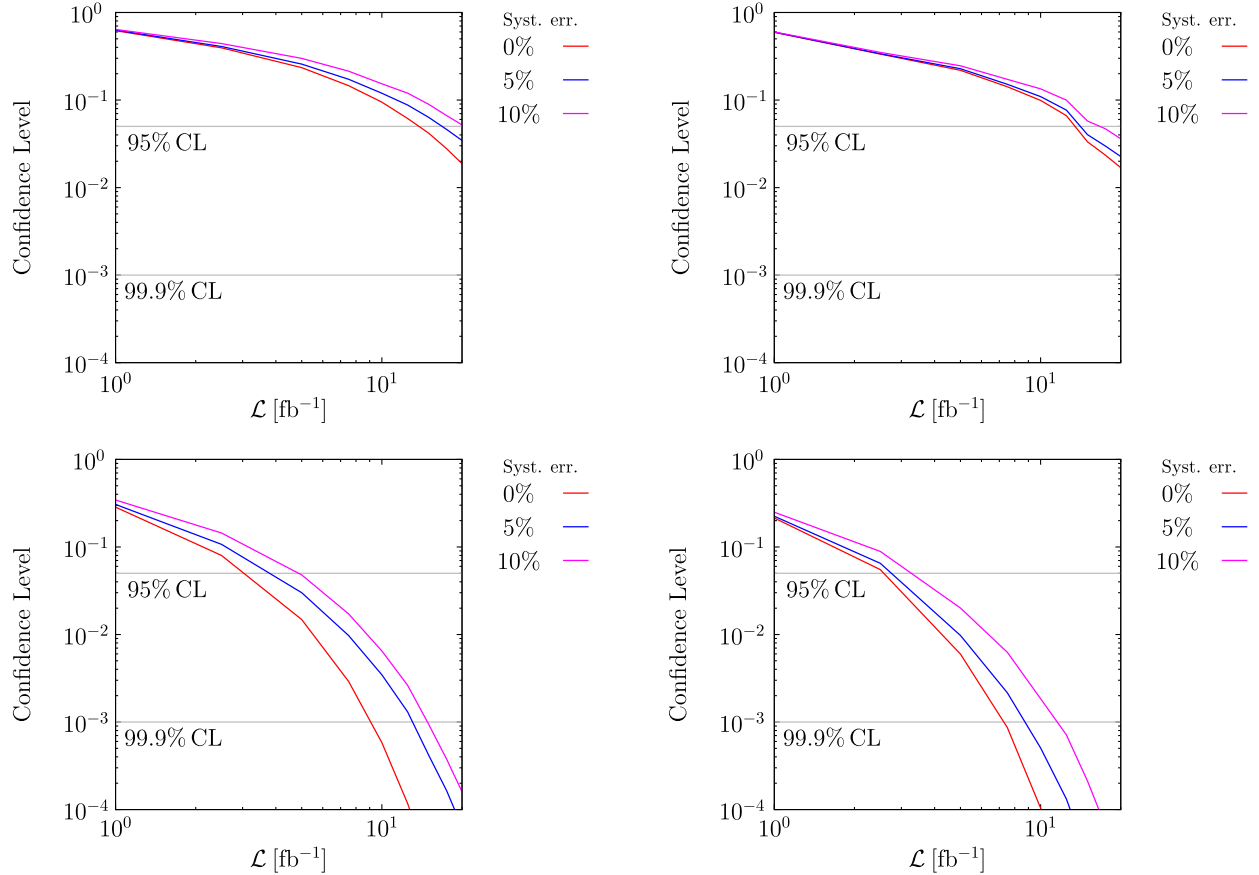


FIG. 3 (color online). The results of the limit-setting procedure when applied to the search for a 700 GeV \tilde{T} using 8 TeV (top) and 14 TeV (bottom) data. The results without requiring a forward jet (left) can be directly compared to the results with a forward jet requirement (right).

20 fb^{-1} integrated luminosity at the 8 TeV LHC. The signal distributions peak close to the \tilde{T} mass while background distributions turn over at lower masses.

A comparison was made with the strategy presented in Ref. [37], where the authors address the Wb final state by using a high p_T lepton, large summed transverse momentum (H_T) and the masses of combinations of final state particles. After running both selections on two signal samples with masses of 700 and 800 GeV, it was found that although the S/\sqrt{B} for both analyses is comparable, our approach accepts between 50% and 70% more events. This will either allow for additional cuts to purify the final state or in an improved reach of the resonance mass or smaller production cross section.

III. RESULTS

In order to estimate whether a singly-produced top partner can be excluded with data collected at the LHC, we use a binned log-likelihood hypothesis test as described in Ref. [38]. The results of this procedure, as a function of integrated luminosity for 8 TeV and 14 TeV LHC data, are presented in Fig. 3, which shows the confidence level at

which single production of a 700 GeV \tilde{T} quark can be excluded in the absence of signal. These results are shown both before and after the forward-jet requirement and for different assumed levels of systematic uncertainty on the backgrounds: 0%, 5% and 10%. It can be seen that the sensitivity is improved by the forward-jet requirement and that the full selection is sufficient to exclude the single-top partner production using 8 TeV data even for the most pessimistic assumed systematic uncertainty. Although this systematic treatment is rather simplistic we expect the search strategy to retain sufficient sensitivity to exclude the 700 GeV T if deployed in a real experimental analysis. For 14 TeV data, the exclusion of the full 8 TeV data set is already surpassed at an integrated luminosity of 5 fb^{-1} .

IV. SUMMARY, CONCLUSIONS AND OUTLOOK

This is the first study to demonstrate a simple and feasible strategy for discovering single production of a top partner in the $\tilde{T} \rightarrow Wb$ channel. The study shows that use of a forward jet and the requirement of a low-mass central large-radius jet and central jet veto are powerful tools for rejecting the SM background processes whilst retaining

acceptable signal efficiency. This analysis is indicative that single production of 700 GeV top partners could be excluded already at the 8 TeV LHC. The mass reach of searches at higher-energy LHC running is likely to be significantly extended. This study considers \tilde{T} production within a specific composite Higgs scenario. However, the analysis is generic and its applicability to top partner searches in other models can be inferred from the production cross sections in our chosen model and from the exclusion limits shown in Fig. 3. We reserve study of $\tilde{T} \rightarrow tH$ and $\tilde{T} \rightarrow tZ$ for a future work, noting that in most searches the extra efficiency in a dominant decay channel outweigh signal purity in the selected sample.

ACKNOWLEDGMENTS

We thank Andy Buckley and Karl Nordstrom for assistance with Rivet, Frank Siegert for advice on SHERPA configuration, and Andrew Pickford for computing support. We thank Oleskii Matsedonskyi, Andrea De Simone and Andrea Wulzer for providing valid parameter points for the composite Higgs scenarios under consideration. We thank Tony Doyle for useful discussion. The work of J. F. and D. K. is supported by the UK Science and Technology Facilities Council (STFC). The work of N. G. is supported by the Scottish Universities Physics Alliance (SUPA).

-
- [1] G. Aad *et al.* (ATLAS Collaboration), *Phys. Lett. B* **716**, 1 (2012).
- [2] S. Chatrchyan *et al.* (CMS Collaboration), *Phys. Lett. B* **716**, 30 (2012).
- [3] H. Georgi and D.B. Kaplan, *Phys. Lett.* **145B**, 216 (1984).
- [4] D.B. Kaplan and H. Georgi, *Phys. Lett.* **136B**, 183 (1984).
- [5] D.B. Kaplan, H. Georgi, and S. Dimopoulos, *Phys. Lett.* **136B**, 187 (1984).
- [6] M.J. Dugan, H. Georgi, and D.B. Kaplan, *Nucl. Phys.* **B254**, 299 (1985).
- [7] R. Contino, Y. Nomura, and A. Pomarol, *Nucl. Phys.* **B671**, 148 (2003).
- [8] K. Agashe, R. Contino, and A. Pomarol, *Nucl. Phys.* **B719**, 165 (2005).
- [9] R. Contino, T. Kramer, M. Son, and R. Sundrum, *J. High Energy Phys.* 05 (2007) 074.
- [10] D.B. Kaplan, *Nucl. Phys.* **B365**, 259 (1991).
- [11] A. De Simone, O. Matsedonskyi, R. Rattazzi, and A. Wulzer, *J. High Energy Phys.* 04 (2013) 004.
- [12] R. Barbieri, B. Bellazzini, V. S. Rychkov, and A. Varagnolo, *Phys. Rev. D* **76**, 115008 (2007).
- [13] G. F. Giudice, C. Grojean, A. Pomarol, and R. Rattazzi, *J. High Energy Phys.* 06 (2007) 045.
- [14] C. Grojean, O. Matsedonskyi, and G. Panico, *J. High Energy Phys.* 10 (2013) 160.
- [15] G. Aad *et al.* (ATLAS Collaboration), *Phys. Lett. B* **718**, 1284 (2013).
- [16] S. Chatrchyan *et al.* (CMS Collaboration), *Phys. Lett. B* **729**, 149 (2014).
- [17] O. Matsedonskyi, G. Panico, and A. Wulzer, *J. High Energy Phys.* 01 (2013) 164.
- [18] J. A. Aguilar-Saavedra, R. Benbrik, S. Heinemeyer, and M. Pérez-Victoria, *Phys. Rev. D* **88**, 094010 (2013).
- [19] J. Mrazek and A. Wulzer, *Phys. Rev. D* **81**, 075006 (2010).
- [20] N. Vignaroli, *Phys. Rev. D* **86**, 075017 (2012).
- [21] E. Álvarez, L. Da Rold, and J.I. Sanchez Vietto, *J. High Energy Phys.* 02 (2014) 010.
- [22] A. Azatov, M. Salvarezza, M. Son, and M. Spannowsky, *Phys. Rev. D* **89**, 075001 (2014).
- [23] J. Alwall, M. Herquet, F. Maltoni, O. Mattelaer, and T. Stelzer, *J. High Energy Phys.* 06 (2011) 128.
- [24] T. Sjostrand, S. Mrenna, and P.Z. Skands, *Comput. Phys. Commun.* **178**, 852 (2008).
- [25] T. Gleisberg, S. Hoeche, F. Krauss, M. Schonherr, S. Schumann, F. Siegert, and J. Winter, *J. High Energy Phys.* 02 (2009) 007.
- [26] J.M. Campbell, R. Frederix, F. Maltoni, and F. Tramontano, *Phys. Rev. Lett.* **102**, 182003 (2009); R. Frederix, E. Re, and P. Torrielli, *J. High Energy Phys.* 09 (2012) 130.
- [27] P. Nason, *J. High Energy Phys.* 11 (2004) 040; S. Frixione, P. Nason, and C. Oleari, *J. High Energy Phys.* 11 (2007) 070; S. Alioli, P. Nason, C. Oleari, and E. Re, *J. High Energy Phys.* 06 (2010) 043.
- [28] M. Cacciari, M. Czakon, M. Mangano, A. Mitov, and P. Nason, *Phys. Lett. B* **710**, 612 (2012); P. Bärnreuther, M. Czakon, and A. Mitov, *Phys. Rev. Lett.* **109**, 132001 (2012); M. Czakon and A. Mitov, *J. High Energy Phys.* 12 (2012) 054; 01 (2013) 080; M. Czakon, P. Fiedler, and A. Mitov, *Phys. Rev. Lett.* **110**, 252004 (2013); M. Czakon and A. Mitov, *Comput. Phys. Commun.* **185**, 2930 (2014).
- [29] M. Czakon, M. L. Mangano, A. Mitov, and J. Rojo, *J. High Energy Phys.* 07 (2013) 167; R. D. Ball *et al.*, *Nucl. Phys.* **B867**, 244 (2013).
- [30] A. Buckley, J. Butterworth, D. Grellscheid, H. Hoeth, L. Lönnblad, J. Monk, H. Schulz, and F. Siegert, *Comput. Phys. Commun.* **184**, 2803 (2013).
- [31] G. Aad *et al.* (ATLAS Collaboration), *J. High Energy Phys.* 12 (2012) 007.
- [32] G. Aad *et al.* (ATLAS Collaboration), *J. High Energy Phys.* 09 (2010) 056.
- [33] M. Cacciari, G.P. Salam, and G. Soyez, *J. High Energy Phys.* 04 (2008) 063.

- [34] M. Cacciari, G. P. Salam, and G. Soyez, *Eur. Phys. J. C* **72**, 1896 (2012).
- [35] G. Aad *et al.* (ATLAS Collaboration), *Phys. Rev. D* **88**, 012004 (2013).
- [36] C. F. Berger, C. Marcantonini, I. W. Stewart, F. J. Tackmann, and W. J. Waalewijn, *J. High Energy Phys.* 04 (2011) 092;
- A. Banfi, P. F. Monni, G. P. Salam, and G. Zanderighi, *Phys. Rev. Lett.* **109**, 202001 (2012).
- [37] J. Li, D. Liu, and J. Shu, *J. High Energy Phys.* 11 (2013) 047.
- [38] T. Junk, *Nucl. Instrum. Methods Phys. Res., Sect. A* **434**, 435 (1999).